applied sciences

MDPI

Article

Zeolitization of Diatomite Residues by a Simple Method

José Manuel Moreno-Maroto [1,2,*], Jacinto Alonso-Azcárate [3], Carmen Martínez-García [2], Maximina Romero [4], Aurora López-Delgado [4] and Teresa Cotes-Palomino [2]

[1] Department of Geology and Geochemistry, Faculty of Sciences, Autonomous University of Madrid, Cantoblanco, 28049 Madrid, Spain
[2] Department of Chemical, Environmental and Materials Engineering, Higher Polytechnic School of Linares, Scientific and Technological Campus of Linares, University of Jaén, 23700 Linares (Jaén), Spain
[3] Department of Physical Chemistry, Faculty of Environmental Sciences and Biochemistry, University of Castilla-La Mancha, Avenida Carlos III, s/n, 45071 Toledo, Spain
[4] Eduardo Torroja Institute for Construction Sciences, IETcc-CSIC, 28033 Madrid, Spain
* Correspondence: josemanuel.moreno@uam.es

Abstract: The possibility of transforming a diatomite-rich waste from the brewing industry into synthetic zeolites has been investigated. After precalcination at 550 °C to eliminate the retained organic matter, the clean diatomite (Dt; with a Si/Al molar ratio of 17.4), was hydrothermally treated for 24 h with continuous stirring in a 3M NaOH solution at 80 °C. The results of mineralogical characterization by X-ray diffraction with Rietveld refinement have shown a crystallization of 55% of zeolite P, which was neoformed from the amorphous phase, opal-CT and quartz of the starting sample. The spectra obtained by Fourier Transform Infrared Spectrometry have corroborated such zeolitization. N_2 adsorption–desorption isotherms have shown that the zeolitized material (Dt-Z) is mesoporous, with almost 60% more specific surface area than Dt (62.6 m^2/g vs. 39.4 m^2/g), greater microporosity and 40% smaller average pore size than Dt (71 Å vs. 118 Å). This study is a first approximation to know the potential of diatomite wastes as zeolite precursors, for which additional research including an aluminum source will be required.

Keywords: zeolite; diatomite; waste valorization; hydrothermal synthesis; NaOH

check for updates

Citation: Moreno-Maroto, J.M.; Alonso-Azcárate, J.; Martínez-García, C.; Romero, M.; López-Delgado, A.; Cotes-Palomino, T. Zeolitization of Diatomite Residues by a Simple Method. *Appl. Sci.* **2022**, *12*, 10977. https://doi.org/10.3390/app122110977

Academic Editors: Theodore E. Matikas and Nikolaos Koukouzas

Received: 8 September 2022
Accepted: 28 October 2022
Published: 29 October 2022

Publisher's Note: MDPI stays neutral with regard to jurisdictional claims in published maps and institutional affiliations.

Copyright: © 2022 by the authors. Licensee MDPI, Basel, Switzerland. This article is an open access article distributed under the terms and conditions of the Creative Commons Attribution (CC BY) license (https://creativecommons.org/licenses/by/4.0/).

1. Introduction

Diatomite, also called diatomaceous earth, is a type of sedimentary rock formed by the fossilization of unicellular algae called diatoms. Its composition is mainly rich in hydrated amorphous or opaline silica, being chemically stable and inert. The holed structural pattern of diatomite gives it very interesting physical properties, which has led this material to be commonly used in different industrial processes as an absorbent, filter medium, thermal insulator, filler, catalyst carrier, among others [1,2]. Accordingly, diatomite has been exploited for more than a century and is used in large quantities due to its low cost [3,4]. Among other applications, diatomite is used in the agri-food industry as a filter medium in the production of wine and beer, generating large quantities of waste rich in this material, in this case saturated in organic matter. From an environmental and economic perspective, different strategies are being considered to valorize these wastes, not only to obtain new products with added value, but also to reduce their potential hazardousness [3,4].

Among the potential options is the possibility of synthesizing zeolites from raw materials rich in diatomite, preferably in residual form. Zeolites are microporous aluminosilicate minerals, made up of TO_4 tetrahedrons (where T is Si or Al) assembled with oxygen bonds. Zeolites, whether natural or synthesized, present a wide variety of nanoporous crystalline structures with interconnected cages. Due to their nanostructure, zeolites can be considered advanced materials whose application is very wide as a catalyst in chemical

processes, adsorbent of cations and organic molecules, desalination processes, gas separation, etc. [4,5]. There are several publications that cover the study of the synthesis of zeolites from (fundamentally natural) diatomites, some of which are summarized below.

Shan et al. [6] manufactured (Fe,Al)-ZSM-5 zeolite microspheres with meso- and macroporosity from natural diatomite, using different reagents (NaOH, tetrapropylammonium bromide (TPABr), NaCl and distilled water). The zeolite was hydrothermally synthesized in an autoclave for 6 days at 180 °C, with subsequent removal of TPABr by calcination at 550 °C. Paper sludge ash in combination with different proportions of diatomite as silica source were used by Wajima et al. [7] to obtain zeolite Na-P1 (zeolite P). The zeolite crystallization process was carried out by hydrothermal means in an Erlenmeyer flask for 24 h at 90 °C, using a 3M NaOH solution as alkaline medium. The zeolite obtained presented the capacity to eliminate NH_4^+ and PO_4^{3-}, having potential application in water filtration. Jia et al. [8] produced zeolites with hierarchical porosity from a commercial diatomite. Once several steps were completed, the final zeolitization process was carried out in an autoclave at 150 °C for 72 h. After applying a scrubbing treatment on a commercial diatomite in order to remove impurity phases, Du et al. [9] synthesized zeolite P using NaOH, $Al(OH)_3$ and deionized water as chemical reagents. The zeolitization was carried out by the authors using a water bath at 90 °C, studying different treatment times (4–24 h).

For their part, Yao et al. [10] used a commercial diatomite, NaOH and $Al(OH)_3$ to synthesize zeolite X. After a first stage of aging at different times and temperatures between 0–120 min and 30–60 °C, zeolites were obtained by hydrothermal treatment also studying different conditions, between 90–120 °C and 3–9 h. Servatan et al. [11] synthesized mesoporous zeolites using a diatomite exploited in an Iranian mine. The synthesis process covered different stages, including, precalcination; acid treatment; treatment with TPABr, sodium aluminate and NaOH; hydrothermal treatment at 170 °C for 60 h; treatment with NH_4NO_3 and final calcination. As a result, the authors obtained ZSM-5 zeolites of good quality. In a relatively recent study, Stafin et al. [4] used diatomaceous earth wastes from beer filtration. Apart from distilled water, the diatomite was mixed with NaOH and $Al(NO_3)_3 \cdot 9H_2O$ as aluminum source. Both a conventional hydrothermal treatment route (100 °C at different times between 3 and 24 h) and through microwaves for 170 s were investigated. Zeolite NaP1, hydrosodalite, sodalite and cancrinite were obtained as products of interest, concluding that microwave treatment can also be very effective.

The present study aims to deepen the knowledge of the synthesis of zeolites from diatomite. In this case, a primary route to know the potential of diatomite wastes as zeolite precursors will be looked for. If adequate, it will pave the way for additional research to obtain quality zeolites from diatomite wastes. It will be especially relevant the non-addition of any aluminum source, so that, unlike what has been presented so far in the literature, silicon-rich diatomaceous earths will be used as the only precursor in the zeolite synthesis. Furthermore, considering the current guidelines of sustainability and circular economy, another of the main objectives is not to use natural raw materials, so the feasibility of a residual diatomite from the brewing industry will be studied as a precursor in zeolitization.

2. Materials and Methods

The diatomite residue used in this investigation came from the filter earths used in the beer brewing process of the Heineken company at its plant located in Jaén (Spain). Once dried in an oven at 105 °C, this material was ready to be used without the need for grinding, since its particle size presented a high fineness (all the material passed through the 63-µm sieve). Thus, the energy and economic costs of milling would be eliminated, an aspect that is especially positive if the zeolitization protocol described were to be scaled up to an industrial level. The diatomite's chemical composition (obtained by X-ray fluorescence using a Thermo ARL ADVANT'XP Sequential XRF equipment) is shown in Table 1.

Table 1. Chemical composition of the diatomite residue used in this research as received and after calcination at 550 °C (data in percentage).

Diatomite	SiO_2	Al_2O_3	Fe_2O_3	K_2O	MgO	CaO	TiO_2	Na_2O	P_2O_5	SO_3	LOI
As received	76.8	3.8	1.5	1.0	0.2	0.8	0.4	0.7	0.3	0.03	14.5
Calcined (Dt)	89.8	4.4	1.8	1.1	0.2	0.9	0.4	0.8	0.4	0.03	0.0

The high percentage of loss on ignition (LOI) is attributable to the organic matter retained in the diatomite mineral matrix during the filtration process in beer production. Accordingly, the diatomite waste was calcined at 550 °C for 5 h in a muffle to remove the organic matter. On the other hand, as expected, the SiO_2 content is predominant, reaching a value of almost 90% after calcination (Table 1), since silicon is the main component of diatomaceous earths. Far below, the second element present is aluminum (~4%), followed by lower proportions of iron and alkali and alkaline earth metals, among others. The presence of these elements could be due to impurities in the diatomite itself, as well as to substances retained in its structure during filtration. Despite this, the chemical composition of Table 1 is in the same order as others found in the literature for diatomaceous earths from different sources and countries [12]. As a result, the Si/Al molar ratio of the raw material is high (Si/Al = 17.4).

After that, the clean diatomite (Dt) was subjected to hydrothermal treatment with a 3M NaOH solution. The liquid (NaOH solution)/solid (mass of Dt) ratio used was 10, specifically 10 g of Dt in 100 mL of NaOH solution. The mixture was kept under constant magnetic stirring for 24 h at 80 °C in a closed Erlenmeyer flask [7]. On completion of the 24 h of hydrothermal stirring, the suspension was filtered and washed with distilled water until a neutral pH was reached. The sediment finally obtained was dried at 105 °C in an oven and subsequently characterized. The sample obtained after this treatment was named Dt-Z.

The quantitative mineralogical composition of the original Dt and the phases formed from it was determined by X-ray diffraction (XRD) using a PANalytical® diffractometer X'Pert Pro model. For this analysis, polycrystalline powder diffractograms were obtained after adding ~25 wt.% alumina to the sample in order to determine both the crystalline and amorphous phases by Rietveld refinement [13,14]. The measurement conditions were as follows: 45 kV, 40 mA, Cu radiation, soller slit of 0.04 rad, antiscattering slit of 1/2°, divergence slit of 1/8°, step size of 0.0167, counting time (s) of 130, Bragg-Brentano HD module and X'celerator detector. The Rietveld analysis of the sample was carried out with the HSP program of Panalytical. It is important to note that the quantification of mineral/amorphous phases is not an aspect usually addressed in other studies shown in the literature, which are limited exclusively to phase identification, making this a point of special interest in this research. The N_2 adsorption–desorption isotherms at 77 K of both Dt and the resulting zeolites (Dt-Z) were obtained using Surface Area and Porosity Analyzer–Model ASAP 2420 manufactured by Micromeritics Instrument Corporation, deducing the Brunauer–Emmett–Teller (BET) surface area, the Barrett–Joyner–Halenda (BJH) mesopore characteristics, as well as the micropore volume based on the Density Functional Theory (DFT). The chemical bonds generated during the zeolitization was studied by Fourier Transform Infrared Spectrometry (FTIR) using a Bruker Vertex 70v equipment, applying the Attenuated Total Reflection (ATR) method. The spectra were obtained between 4000 and 400 cm^{-1} and a resolution of 2 cm^{-1}.

3. Results and Discussion

3.1. XRD Analysis: Mineralogical Transformations

Figure 1 shows the diffractograms obtained from the XRD test applied to Dt and Dt-Z, while a summary of the quantification by Rietveld method of the different phases is shown in Table 2. The diatomite used in this research has a fundamentally amorphous nature (81.2%), which makes it a material with, a priori, good zeolitization potential. Considering

the chemical composition shown in Table 1, such an amorphous phase would be mainly composed of SiO_2. In smaller proportions, Dt also presents opal-CT (11.1%) and quartz (7.7%) as the only crystalline phases present in the original sample. However, as can be seen in Figure 1 and Table 2, the alkaline hydrothermal treatment has produced very significant changes both in the proportions of these original phases and in the neoformation of new ones. Thus, Dt-Z contains only 39.2% and is amorphous phase; it does not contain opal-CT and its quartz proportion has also been reduced to 4.3 %. In addition, new minerals have crystallized. As a minor species, calcite (1.6%) has been neoformed, whose crystallization could have been due to the presence of Ca^{2+} ions that have reacted with dissolved CO_2 during the hydrothermal agitation. However, calcite's contribution to the mineralogy of Dt-Z is not very relevant if compared to zeolite-P, whose crystallization fulfills the objective of this research, also being the predominant phase in Dt-Z, representing 55% of the total sample.

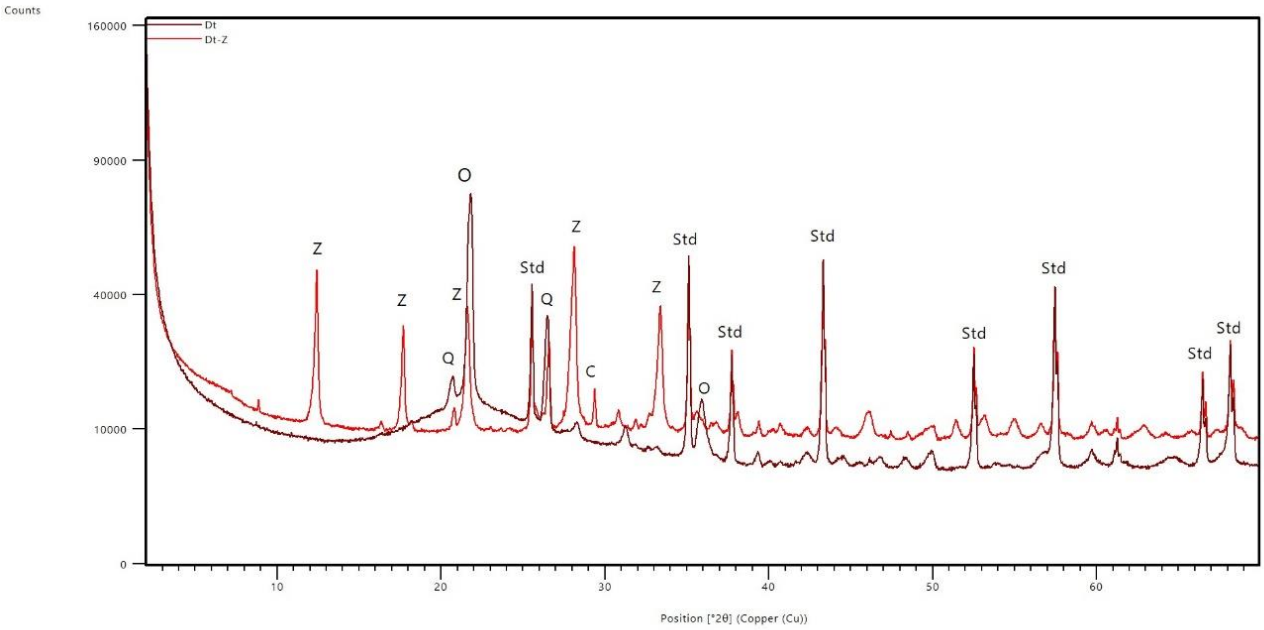


Figure 1. XRD diagrams of Dt and Dt-Z. Q = Quartz; O = Opal-CT; Std = Standard (Al_2O_3); C = Calcite; Z = Zeolite P.

Table 2. Quantitative mineralogical composition of the diatomite (Dt) and the material obtained after hydrothermal treatment (Dt-Z). Data in percentage. Δ % represent the percentage.

	Amorphous	Opal-CT	Quartz	Calcite	Zeolite P
Dt	81.2	11.1	7.7	–	–
Dt-Z	39.2	–	4.3	1.6	54.9
Δ %	−52.8	−100.0	−44.2	100.0	100.0

Based on the database of zeolite structures published by the International Zeolite Association (IZA), zeolite P presents a GIS framework type [15–17], i.e., this is a zeolite topologically related to the mineral called gismondine, presenting a two-dimensional pore system with two intersecting eight-membered oxygen ring channels [15,16]. Although increasingly in disuse compared to other zeolites, due to this structure, zeolite P has potential applications as a separator and adsorbent both at the industrial level and in environmental technologies [7,9,18].

Considering that calcite does not contain silicon in its structure, the zeolite P developed in this investigation would not have been formed solely from the chemical dissolution of the amorphous phase, but also from opal-CT and quartz, minerals that in theory could present

greater difficulties for it. In fact, according to the data in Table 2, the alkaline treatment has been totally effective in dissolving the opal-CT in its entirety, while the original amorphous phase has been wiped out by 52.8% and the quartz by 44.2%. These results refute what has been published by other authors, such as Du et al. [9], who synthesized zeolite P also from diatomite after previously removing all crystalline SiO_2 by considering that the latter could not intervene in zeolite formation, something that is not the case in this study. Although opal-CT could have contributed all its SiO_2 in the neoformation of zeolite P, its original proportion is relatively low, so the amorphous phase can be considered as the one that has released the most silicon involved in the zeolitization of the diatomite. However, on the other hand, it should be noted that the volume of sediment obtained through the hydrothermal synthesis was significantly lower than that of the raw material used. This would indicate that zeolitization has been restricted, a priori, by the low aluminum content of the diatomite and that, therefore, further investigation would be required including some source of aluminum to react with the dissolved silicon.

3.2. N_2 adsorption–Desorption Isotherms: Porosity and Surface Area

The graphs obtained from the N_2 adsorption–desorption isotherms test are shown in Figure 2. In the case of the Dt adsorption curve (Figure 2a), a slight increase in the amount of N_2 adsorbed is observed when the relative pressure is practically zero, and then the adsorption increases at a low rate until approximately P/Po = 0.7. Above this relative pressure, the adsorption rate increases up to about P/Po = 0.95, above which the slope of the curve is again somewhat reduced. In the case of the Dt-Z adsorption curve (Figure 2b), the pathway is similar to that of the Dt sample, with the largest differences observed when P/Po > 0.7, with a less pronounced rise in the rate of adsorbed amount and no final deceleration if compared with Dt. Despite this, during desorption a hysteresis loop is observed for both Dt and Dt-Z, decoupling from the adsorption curve from relative pressures of approximately 0.7 to 0.95 for Dt, and 0.5 to 0.95 for Dt-Z.

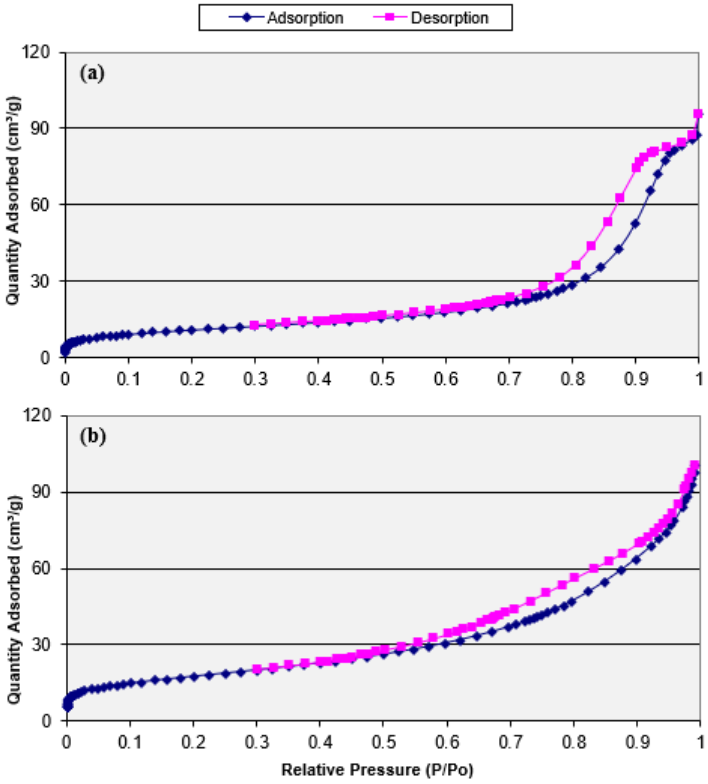


Figure 2. N_2 adsorption–desorption isotherms of: (**a**) initial diatomite, Dt; (**b**) the material obtained after the zeolitization, Dt-Z.

The International Union of Pure and Applied Chemistry (IUPAC) defines six possible types of adsorption isotherms, from which the type of the dominant porosity (if any) in the sample can be deduced [19–22]. The Dt and Dt-Z isotherms would be classified within type IV, typical of mesoporous materials, i.e., in theory, they would present a predominance of pores with sizes between 2 and 50 nm according to the IUPAC [22,23]. In the case of Dt, this type of isotherm (Figure 2a) differs from others for diatomites presented in the literature [8], which show type I isotherms, typical of non-porous or macroporous materials. Probably, the pretreatment at 550 °C may have helped to unclog the micro- and mesopores in Dt, hence their curves show a different trajectory than expected. From the four types of hysteresis loops classified by IUPAC [19,20,22], Dt presents the H1 type, which is typical of materials with well-defined cylindrical-type porous channels or agglomerates of more or less uniform spheres. For its part, Dt-Z exhibits an H3-type hysteresis loop, which is usually linked to slit-shaped pores and non-rigid aggregates of plate-like particles [22].

The main characteristics deduced from the N_2 isotherms test are summarized in Table 3. As can be seen, the alkaline hydrothermal treatment has produced a substantial increase in the specific surface area according to the BET method. S_{BET} has increased from 39.4 m^2/g for Dt to 62.6 m^2/g for Dt-Z, which in percentage terms is almost a 60% increase in specific surface area. This specific surface area value is slightly higher than the maximum S_{BET} obtained by Du et al. [9] in zeolites P also produced from diatomites (59.5 m^2/g) by using a more laborious method, which also included the addition of an aluminum source.

Table 3. Main properties deduced from N_2 adsorption–desorption isotherms.

	S_{BET} (m^2/g)	DFT Micro (cm^3/g)	BJH Cumulative Pore Volume (cm^3/g)			BJH Average Pore Width (Å)		
			Adsorption	Desorption	Average	Adsorp.	Desorp.	Average
Dt	39.38	0.002	0.11	0.13	0.12	121.8	114.0	117.9
Dt-Z	62.57	0.005	0.10	0.13	0.11	67.8	74.3	71.0
Δ%	58.9	124.6	−10.9	0.5	−4.9	−44.4	−34.8	−39.7

NOTE: S_{BET} = specific surface area calculated according to the BET theory; DFT micro = microporosity volume calculated according to the DFT theory, considering the cumulative pore volume < 20 Å. BJH results embrace both micro- and mesoporosity.

Returning to the results of the present investigation, although the microporosity (represented in this case as the accumulated volume of pores smaller than 2 nm) is not too high in either sample, an increase is again observed, from 0.002 cm^3/g in Dt to more than double in Dt-Z (0.005 cm^3/g). However, the data estimated from the BJH method indicate that the total pore volume has hardly varied between both samples, even decreasing slightly (−4.9%) this property in the Dt-Z sample with respect to the untreated diatomite. The fact that the volume of accumulated porosity has hardly changed when applying the hydrothermal treatment, while the specific surface area has increased is an indicator that there has been a change in the pore size, so that in Dt-Z the pores would present a smaller size, being also more numerous than in Dt as a result of the zeolitization process (Figure 3). This is demonstrated not only in the increase in microporosity just mentioned, but also in the mean pore size estimated with the BJH theory (Table 3), showing a reduction in pore size of almost 40%, from 118 Å in Dt to 71 Å in Dt-Z (Figure 3).

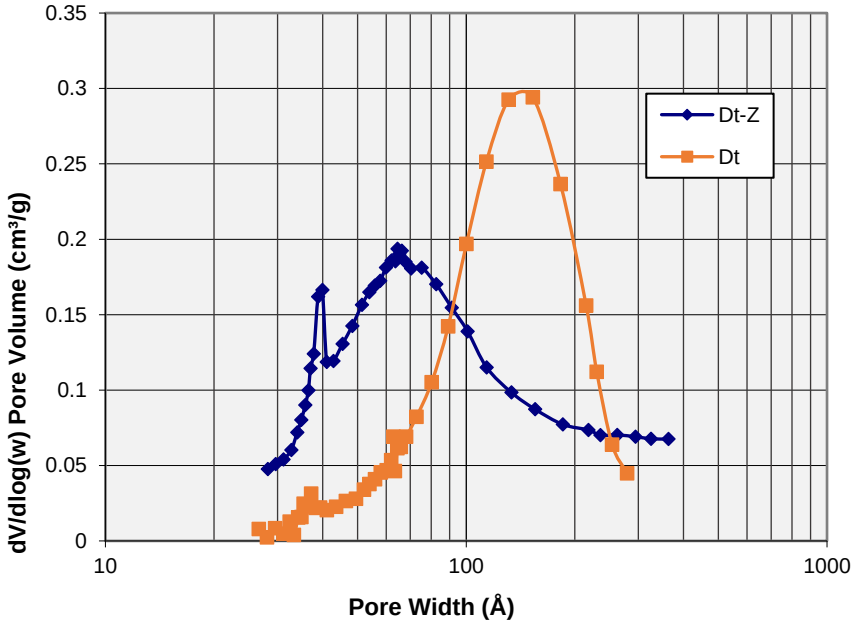


Figure 3. BJH Desorption dV/dlog(w) Pore Volume vs. Pore Width for Dt and Dt-Z.

Although there is a predominance of mesoporosity over microporosity, as explained in the previous section, according to the results of Figure 1 and Table 2, zeolitization of Dt has been effectively carried out. In fact, this is consistent with other works already published that show the obtaining of mesoporous zeolites from diatomite, such as that of Servatan et al. [11] or the previously cited of Du et al. [9]. However, it should be noted that the volume of sediment obtained was significantly lower than that of the raw material used. This would indicate that zeolitization has been restricted, a priori, by the low aluminum content of the diatomite and that, therefore, further investigation would be required including some source of aluminum to react with the dissolved silicon.

3.3. FTIR Results: Endorsing the Findings on Zeolitization

The diagrams obtained by FTIR spectra are shown in Figure 4. Between 2950–3600 cm^{-1} there is a slight variation in the absorbance of Dt-Z which is practically negligible for Dt. This band is related to hydration, namely to the H-O-H vibrations of stretching and bending of the free water molecules, as well as those absorbed in the pores and adsorbed on the particles' surface [24–26]. Similarly, at 1597 cm^{-1} there is a band in Dt-Z, which is not observed in Dt, and is attributable to the bending of water molecules bound to the zeolite particles [2,27].

At 1044 cm^{-1} a band of high intensity is observed in Dt, which is associated with asymmetric bending/stretching vibrations in T-O-(T) bonds, where T is Si or Al [11,28,29]. Considering the chemical composition of the Dt sample (Table 1), it is expected that T is mostly silicon. In the case of Dt-Z this band appears somewhat shifted towards smaller wavelengths, specifically at 957 cm^{-1}. According to Milkey [30], this displacement towards shorter wavelengths could be directly related to the inclusion of Al atoms in the T-O-T bonds, to give rise not only to Si-O-Si bonds, but also Si-O-Al ones during the formation of the zeolite P obtained. However, it must be taken into account that the sample used has a low percentage of aluminum (3.8%; Table 1) and that no reagent has been incorporated to increase its content, so that this type of Si-O-Al bonds would be, in theory, less representative.

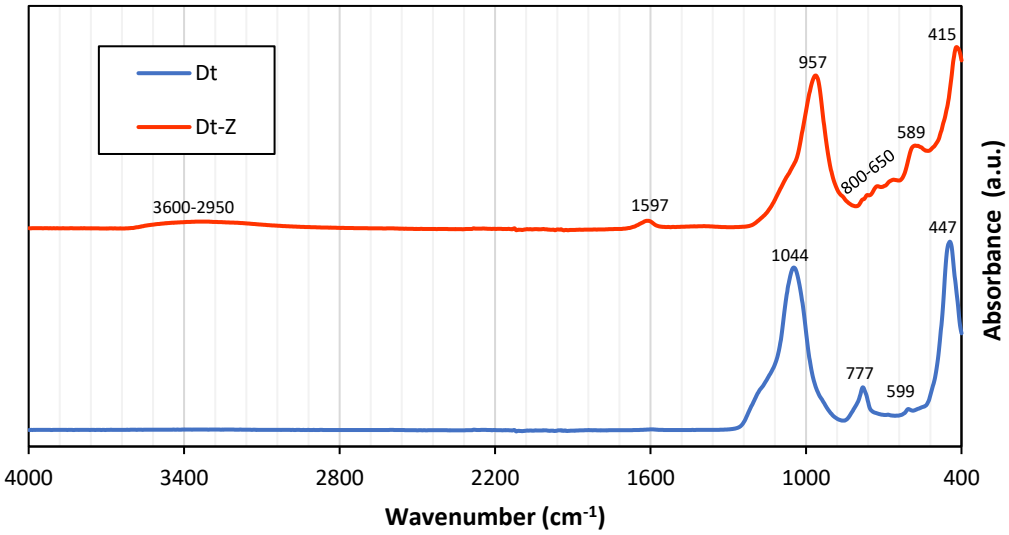


Figure 4. FTIR spectrum bands of the diatomite waste (Dt) and the material obtained after the hydrothermal synthesis (Dt-Z).

In the wavelength range between approximately 400 and 800 cm^{-1}, a series of peaks are seen that differ depending on the sample. In the non-hydrothermally treated diatomite, bands at 777 cm^{-1} and 447 cm^{-1} stand out, with the presence also of a very low intensity band at 599 cm^{-1}. In contrast, the zeolitization process in Dt-Z is mainly associated with a band at 589 cm^{-1} (of much higher intensity than that observed in Dt at 599 cm^{-1}) and another at 415 cm^{-1} (again shifted towards lower wavelengths with respect to that observed in Dt at 447 cm^{-1}), while between 650–800 cm^{-1} there is a succession of small peaks of low intensity, with no evidence of the band at 777 cm^{-1} observed in Dt. All these bands are related to symmetric stretching vibrations of the T-O-T bridge bonds described above, with the exception of the bands at 447 cm^{-1} (Dt) and 415 cm^{-1} (Dt-Z), which are due to bending vibrations in O-Si-O bonds, and to a lesser extent in O-Al-O (in the latter case, linked mainly to the lower wavelengths of Dt-Z) [11,26,28].

Therefore, the FTIR spectra shown in Figure 4 corroborate the changes in the bonds between atoms occurred during the alkaline hydrothermal treatment leading to the formation of zeolite P in the sediment obtained after treating the diatomite without any additional reagents other than NaOH.

4. Conclusions

A simple approach has been presented to investigate the potential of brewing industry diatomite-rich wastes with a Si/Al molar ratio of 17.4 as zeolite precursor. A 24 h hydrothermal treatment was applied using a 3M NaOH solution at low pressure and temperature (80 °C). The main conclusions drawn from this investigation are the following:

- It has been demonstrated that it is possible to synthesize zeolites (in this case zeolite P) from this type of raw materials without the addition of any aluminum supplying component. Despite this, the volume of sediment obtained was significantly lower than that of the raw material used, so further investigation would be required including some source of aluminum to improve the protocol.
- Quantitative XRD tests have shown that the zeolitization process has been effective, forming a material with 55% zeolite P from the hydrothermal transformation of both the amorphous phase, the opal-CT and, to a lesser extent, the quartz present in the original diatomite-rich residue. Such mineralogical transformations have been corroborated through changes in the bands observed in the FTIR spectra.
- The N_2 adsorption–desorption isotherms tests have revealed that although the starting diatomite presented a relatively high specific surface (39.4 m^2/g), the zeolitization treatment has involved a positive effect, increasing this property by almost 60% (62.6 m^2/g).

This specific surface area value is slightly higher than the maximum S_{BET} obtained by Du et al. [9] in zeolites P also produced from diatomites by applying a more laborious method and with the addition of an Al source. Similarly, although the pore volume has hardly changed, the treatment described has favored a reduction in its size by almost 40%, from an average pore size of 118 Å to 71 Å. Therefore, the zeolite formed would be fundamentally mesoporous, like others previously reported in the literature.

- This study shows only a first approach to obtain zeolites from diatomite wastes. Therefore, the findings of this investigation could be useful for future research in order to improve certain properties, such as increasing the purity of the zeolite obtained, increasing its specific surface area and reducing the overall pore size.

Author Contributions: J.M.M.-M.: Conceptualization, investigation, methodology, visualization, writing original draft, writing—review and editing, funding acquisition. J.A.-A.: investigation, writing—review and editing, funding acquisition. M.R. and A.L.-D.: writing—review and editing. C.M.-G. and T.C.-P.: writing—review and editing, funding acquisition. All authors have read and agreed to the published version of the manuscript.

Funding: This research was funded by the Spanish Ministry of Science, Innovation and Universities and ERDF funds through the ECO-MET-AL Project, PID2019-109520RB-I00/AEI/10.13039/501100011033, "Can industrial and mining metalliferous wastes produce green lightweight aggregates? Applying the Circular Economy" framed in the "Ayudas a "Proyectos I+D+i" en el marco de los Programas Estatales de Generación de Conocimiento y Fortalecimiento Científico y Tecnológico del Sistema de I+D+i y de I+D+i orientada a los Retos de la Sociedad, Convocatoria 2019". This research was also funded by the Postdoctoral Contract granted through the Resolution of 21 May 2020, of the General Secretariat for Universities, Research and Technology of the Government of Andalusia (Spain) within the scope of the Andalusian Plan for Research, Development and Innovation (PAIDI 2020).

Acknowledgments: This research was conducted as a part of the ECO-MET-AL Project, PID2019-109520RB-I00/AEI/10.13039/501100011033, "Can industrial and mining metalliferous wastes produce green lightweight aggregates? Applying the Circular Economy" funded by the Spanish Ministry of Science, Innovation and Universities and ERDF funds, framed in the "Ayudas a "Proyectos I+D+i" en el marco de los Programas Estatales de Generación de Conocimiento y Fortalecimiento Científico y Tecnológico del Sistema de I+D+i y de I+D+i orientada a los Retos de la Sociedad, Convocatoria 2019". Thanks also to the SCAI of the University of Jaén, the University of Castilla-La Mancha and the University of Málaga for their services. The authors also acknowledge the Postdoctoral Contract granted through the Resolution of 21 May 2020, of the General Secretariat for Universities, Research and Technology of the Government of Andalusia (Spain) within the scope of the Andalusian Plan for Research, Development and Innovation (PAIDI 2020).

Conflicts of Interest: The authors declare no conflict of interest.

References

1. Biswajit, G.; Dinesh, C.; Subhash, B. Synthesis of zeolite A from calcined diatomaceous clay: Optimization studies. *Ind. Eng. Chem. Res.* **1994**, *33*, 2107–2110. [CrossRef]
2. Chaisena, A.; Rangsriwatananon, K. Effects of thermal and acid treatments on some physico-chemical poroperies of Lampang diatomite. *Suranaree J. Sci. Technol.* **2004**, *11*, 289–299.
3. Fillaudeau, L.; Blanpain-Avet, P.; Daufin, G. Water, wastewater and waste management in brewing industries. *J. Clean. Prod.* **2006**, *14*, 463–471. [CrossRef]
4. Stafin, G.; Grzebielucka, E.C.; Antunes, S.R.; Ferreira Borges, C.P.; Chaves de Andrade, A.V.; Aparecida Alves, S.; Ferreira de Souza, E.C. Synthesis of zeolites from residual diatomite using a microwave-assisted hydrothermal method. *Waste Manag.* **2021**, *126*, 853–860. [CrossRef] [PubMed]
5. Lobo-Recio, M.A.; Rodrigues, C.; Jeremias, T.C.; Lapolli, F.R.; Padilla, I.; López-Delgado, A. Highly efficient removal of aluminum, iron, and manganese ions using Linde type-A zeolite obtained from hazardous waste. *Chemosphere* **2021**, *267*, 128919. [CrossRef]
6. Shan, W.; Zhang, Y.; Wang, Y.; Xia, J.; Tang, Y. Synthesis of Meso-/Macroporous Zeolite (Fe,Al)-ZSM-5 Microspheres from Diatomite. *Chem. Lett.* **2004**, *33*, 270–271. [CrossRef]
7. Wajima, T.; Haga, M.; Kuzawa, K.; Ishimoto, H.; Tamada, O.; Ito, K.; Nishiyama, T.; Downs, R.T.; Rakovan, J.F. Zeolite synthesis from paper sludge ash at low temperature (90 °C) with addition of diatomite. *J. Hazard. Mater.* **2006**, *132*, 244–252. [CrossRef] [PubMed]

8. Jia, Y.; Han, W.; Xiong, G.; Yang, W. A method for diatomite zeolitization through steam-assisted crystallization with in-situ seeding. *Mater. Lett.* **2008**, *62*, 2400–2403. [CrossRef]
9. Du, Y.; Shi, S.; Dai, H. Water-bathing synthesis of high-surface-area zeolite P from diatomite. *Particuology* **2011**, *9*, 174–178. [CrossRef]
10. Yao, G.; Lei, J.; Zhang, X.; Sun, Z.; Zheng, S. One-Step Hydrothermal Synthesis of Zeolite X Powder from Natural Low-Grade Diatomite. *Materials* **2018**, *11*, 906. [CrossRef]
11. Servatan, M.; Ghadiri, M.; Yazdi, M.K.; Jouyandeh, M.; Mahmodi, G.; Samadi, A.; Zarrintaj, P.; Habibzadeh, S.; Ganjali, M.R.; Saeb, M.R. Synthesis of Cost-Effective Hierarchical MFI-Type Mesoporous Zeolite: Introducing Diatomite as Silica Source. *Silicon* **2021**, *13*, 3461–3472. [CrossRef]
12. Danil de Namor, A.F.; El Gamouz, A.; Frangie, S.; Martinez, V.; Valiente, L.; Webb, O.A. Turning the volume down on heavy metals using tuned diatomite. A review of diatomite and modified diatomite for the extraction of heavy metals from water. *J. Hazard. Mater.* **2012**, *241–242*, 14–31. [CrossRef] [PubMed]
13. Bish, D.L.; Post, J.E. Quantitative mineralogical analysis using the Rietveld full pattern fitting method. *Am. Mineral.* **1993**, *78*, 932–940.
14. Moreno-Maroto, J.M.; González-Corrochano, B.; Alonso-Azcárate, J.; Rodríguez, L.; Acosta, A. Assessment of crystalline phase changes and glass formation by Rietveld- XRD method on ceramic lightweight aggregates sintered from mineral and polymeric wastes. *Ceram. Int.* **2018**, *44*, 11840–11851. [CrossRef]
15. IZA. International Zeolite Association (IZA). Database of Zeolite Structures. 2022. Available online: http://www.iza-structure.org/databases/ (accessed on 1 August 2022).
16. Albert, B.R.; Cheetham, A.K.; Adams, C.J. Investigations on P zeolites: Synthesis and structure of the gismondine analogue, highly crystalline low-silica CaP. *Microporous Mesoporous Mater.* **1998**, *21*, 127–132. [CrossRef]
17. Yang, S.; Lach-hab, M.; Vaisman, I.; Blaisten-Barojas, E.; Li, X.; Karen, V.L. Framework-Type Determination for Zeolite Structures in the Inorganic Crystal Structure Database. *J. Phys. Chem. Ref. Data.* **2010**, *39*, 033102. [CrossRef]
18. Baerlocher, C.; Meier, W.M. The crystal structure of synthetic zeolite Na-P 1, an isotype of gismondine. *Z. Für. Krist. -Cryst. Mater.* **1972**, *135*, 339–354. [CrossRef]
19. Broekhoff, J.C.P. Mesopore determination from nitrogen sorption isotherms: Fundamentals, scope, limitations. *Stud. Surf. Sci. Catal.* **1979**, *3*, 663–684.
20. Sing, K.S.W.; Everett, D.H.; Haul, R.A.W.; Moscou, L.; Pierotti, R.A.; Rouquerol, J.; Siemieniewska, T. Reporting physisorption data for gas/solid systems with special reference to the determination of surface area and porosity. *Pure Appl. Chem.* **1985**, *57*, 603–619. [CrossRef]
21. Shields, J.E.; Lowell, S.; Thomas, M.A.; Thommes, M. *Characterization of Porous Solids and Powders: Surface Area, Pore Size and Density*; Kluwer Academic Publisher: Boston, MA, USA, 2004; pp. 43–45.
22. Alothman, Z.A. A Review: Fundamental Aspects of Silicate Mesoporous. *Materials* **2012**, *5*, 2874–2902. [CrossRef]
23. Tangestaninejad, S.; Moghadam, M.; Mirkhani, V.; Baltork, I.M.; Ghani, K. Alkene epoxidation catalyzed by molybdenum supported on functionalized MCM-41 containing N–S chelating Schiff base ligand. *Catal. Commun.* **2009**, *10*, 853–858. [CrossRef]
24. Madejova, J.; Janek, M.; Komadel, P.; Herbert, H.J.; Moog, H.C. FTIR analyses of water in MX-80 bentonite compacted from high salinary salt solution systems. *Appl. Clay Sci.* **2002**, *20*, 255–271. [CrossRef]
25. Ilia, I.K.; Stamatakis, M.G.; Perraki, T.S. Mineralogy and technical properties of clayey diatomites from north and central Greece. *Open Geosci.* **2009**, *1*, 393–403. [CrossRef]
26. Moreno-Maroto, J.M.; Delgado-Plana, P.; Cabezas-Rodríguez, R.; Mejía de Gutiérrez, R.; Eliche-Quesada, D.; Pérez-Villarejo, L.; Galán-Arboledas, R.J.; Bueno, S. Alkaline activation of high-crystalline low-Al_2O_3 Construction and Demolition Wastes to obtain geopolymers. *J. Clean. Prod.* **2022**, *330*, 129770. [CrossRef]
27. Zainal Abidin, A.; Abu Bakar, N.H.H.; Ng, E.P.; Tan, W.L. Rapid Degradation of Methyl Orange by Ag Doped Zeolite X in the Presence of Borohydride. *J. Taibah Univ. Sci.* **2017**, *11*, 1070–1079. [CrossRef]
28. Mozgawa, W.; Król, M.; Barczyk, K. FT-IR studies of zeolites from different structural groups. *Chemik* **2011**, *65*, 667–674.
29. López-Delgado, A.; Robla, J.I.; Padilla, I.; López-Andrés, S.; Romero, M. Zero-waste process for the transformation of a hazardous aluminum waste into a raw material to obtain zeolites. *J. Clean. Prod.* **2020**, *255*, 120178. [CrossRef]
30. Milkey, R.G. Infrared spectra of some tectosilicates. *Am. Mineral.* **1960**, *45*, 990–1007.